Heat-Induced Self-Assembling of Thermosensitive Block Copolymer. Rheology and Dynamic Light Scattering Study

Satoshi Okabe,[†] Shinji Sugihara,[‡] Sadahito Aoshima,[‡] and Mitsuhiro Shibayama*[,†]

Neutron Science Laboratory, Institute for Solid State Physics, The University of Tokyo, Tokai, Ibaraki, 319-1106, Japan, and Department of Macromolecular Science, Graduate School of Science, Osaka University, Toyonaka, Osaka 560-0043, Japan

Received January 27, 2003

ABSTRACT: The dynamic aspects of the thermoreversible morphological transition of poly(2-ethoxyethyl vinyl ether)-*b*-poly(2-hydroxyethyl vinyl ether) (PEOVE-*b*-PHOVE) in aqueous solutions have been investigated by dynamic light scattering (DLS) and rheological measurements. A sample-position-dependent DLS study, employed here, allowed us to resolve two transitions, i.e., (1) molecular dispersion-to-micelle transition and (2) micelle-to-macrolattice transition, which were not clearly resolved by small-angle neutron scattering studies in the previous work. These transitions are characterized by (1) an abrupt increase in the scattered intensity and (2) an appearance of speckle patterns. The temperature where the abrupt increase in intensity was observed was a few degrees lower than that the speckle pattern appeared. Rheological behaviors also supported the two transitions as (1) Newtonian-to-non-Newtonian transition and (2) non-Newtonian-to-plastic flow transition. It is concluded that a pseudo-sol-to-gel transition without chain anchoring is enough for an ergodic-to-nonergodic transition.

Introduction

Block copolymers consisting of unlike block chains provide a variety of nanoorder morphologies, such as spherical, cylindrical, gyroid, and lamellar morphologies, which results in exhibiting fascinating but complicated physical properties.[1] The nanoorder morphologies are one of the most characteristic features of block copolymers called microphase separation. These are fabricated by playing with various combinations of parameters, namely, choice of constituent block chains, their lengths, architecture, and polymer concentration if a solvent is present.[2] The order−disorder transition from a microphase-separated structure to a molecular mixture and order−order transition between different microphase-separated structures have been extensively investigated by electron microscopy, small-angle X-ray scattering, and so on. These transitions have been successively accounted for by molecular theories of block copolymers.[3]

The rheological properties of block copolymer solutions are strongly dependent on their morphologies and phase behavior. For example, the plastic flow to non-Newtonian flow behavior transition and the non-Newtonian to Newtonian flow behavior transition were observed for polystyrene-*b*-polybutadiene (PS-*b*-PB) in *n*-tetradecane (C14) when temperature was raised.[4−6] Here, C14 is a selective solvent for polybutadiene (PB) and a nonsolvent for polystyrene (PS). Small-angle X-ray scattering studies revealed that these transitions are assigned to be lattice ordering and order−disorder transition, respectively. This is an analogy of solid−liquid−vapor phase transitions. In the "solid phase", PS-*b*-PB forms microphase-separated structure with cubic packing of PS spherical domains. As temperature increases, "crystal" melting takes place to liquid phase, where the PS (nonsoluble component) keeps its spherical domain structure as "micelles" with PB corona chains. This is followed by dissolution of PS micelles to a homogeneous polymer solution (liquid-to-vapor transition). Similar structure transitions were also observed in aqueous solutions of polyethylene−polypropylene−polyethylene (PEO-*b*-PPO-*b*-PEO) block copolymers. In this case, PEO-*b*-PPO-*b*-PEO chains are molecularly dispersed in water at low temperatures. When temperature was raised, PPO blocks form micelles with PEO corona. Further heating results in formation of crystalline lattice structure, i.e., "inverse crystallization". The inverse crystallization, meaning crystallization by heating, is due to the hydrophobic nature of PPO, which is commonly observed in hydrophobic polymers in aqueous solutions. The structure transitions were systematically studied by Mortensen by small-angle neutron scattering as a function of temperature and polymer concentration in addition to molecular weights of constituent block chains.[7−9]

A series of block copolymers carrying ether groups in the side chain, e.g., poly(alkyl vinyl ether) with oxyethylene unit as a pendant, are very sensitive to temperature,[10] solvent composition,[11] and so on. These block copolymers are made by living cationic polymerization and have a relatively narrow molecular weight distribution. In our previous paper, we studied structural transitions of poly(2-ethoxyethyl vinyl ether)-*b*-poly(2-hydroxyethyl vinyl ether) (PEOVE-*b*-PHOVE) in aqueous solutions.[12] One of the fascinating phenomena was a thermoreversible sol−gel transition around 20 °C observed in a 17 wt % PEOVE-*b*-PHOVE aqueous solution. The viscosity of the solution changed more than 4 orders of magnitude within a few degrees Celsius. It was found by a series of small-angle neutron scattering (SANS) experiments that this rheological transition is due to morphological transition from a molecular dispersion to a macrolattice structure with a body-centered-cubic structure. Though the SANS study also indicated presence of an intermediate state with micellar structure, it was not decisive because of the limitation of the spatial resolution of SANS.

[†] The University of Tokyo.
[‡] Osaka University.
* To whom correspondence should be addressed.

10.1021/ma030066p CCC: $25.00
Published on Web 05/09/2003

Scheme 1

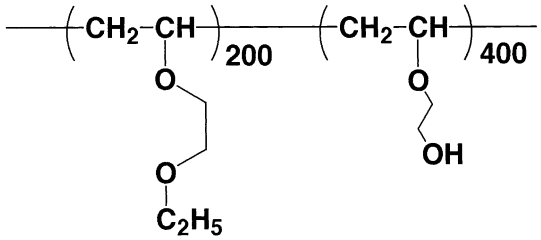

In this paper, we report the dynamics and rheological properties of PEOVE-*b*-PHOVE aqueous solutions as a function of temperature and concentration and confirm the models of morphological transitions proposed in the previous paper.

Theoretical Background

The dynamics of polymer solutions can be analyzed by dynamic light scattering (DLS). Let us first define the normalized first-order correlation function for the scattered electric field $g^{(1)}(\mathbf{q},t)$ from the sample, where $\mathbf{q}$ and t are the scattering vector and time, respectively. $g^{(1)}(\mathbf{q},t)$ is given as follows[13]

$$g^{(1)}(\mathbf{q},\tau) = \frac{\langle E(\mathbf{q},t)\, E^*(\mathbf{q},t+\tau)\rangle}{\langle |E(\mathbf{q},t)|^2\rangle} = \frac{\langle E(\mathbf{q},0)\, E^*(\mathbf{q},\tau)\rangle}{\langle |E(\mathbf{q},0)|^2\rangle} \quad (1)$$

where $E(\mathbf{q},t)$ is the scattering field and $E^*(\mathbf{q},t)$ is the complex conjugate of $E(\mathbf{q},t)$. In a DLS measurement, we obtain the second-order correlation function, $g^{(2)}(\mathbf{q},\tau)$, which is the intensity−intensity−time correlation function defined by

$$g^{(2)}(\mathbf{q},\tau) = \frac{\langle I(\mathbf{q},0)\, I(\mathbf{q},\tau)\rangle}{\langle |I(\mathbf{q},0)|\rangle^2} = \frac{\langle E(\mathbf{q},0)\, E^*(\mathbf{q},0)\, E(\mathbf{q},\tau)\, E^*(\mathbf{q},\tau)\rangle}{\langle |E(\mathbf{q},0)|^2\rangle^2} \quad (2)$$

Here, $I(\mathbf{q},t)$ is the scattered intensity at $\mathbf{q}$ and at time t. The two correlation functions are linked via the Siegert relation,[14,15] i.e.

$$g^{(2)}(q,\tau) = 1 + |g^{(1)}(q,\tau)|^2 \quad (3)$$

In general, there are many relaxation processes, and $g^{(1)}(q,\tau)$ is given with the decay-rate distribution function, $G(\Gamma)$, where Γ is the decay rate

$$g^{(1)}(q,\tau) = \int_0^\infty G(\Gamma) \exp(-\Gamma\tau)\, d\Gamma \quad (4)$$

For example, if the scattering medium has two relaxation modes with monodisperse distributions, $g^{(1)}(q,\tau)$ is simply given as a sum of two exponential functions, i.e.

$$g^{(1)}(q,\tau) = A \exp(-\Gamma_1\tau) + (1 - A) \exp(-\Gamma_2\tau) \quad \text{(two exponentials)} \quad (5)$$

Γ_i ($i = 1, 2$) is the characteristic decay rate related to the diffusion coefficient, D_i, as follows:

$$\Gamma_i = D_i q^2 \quad (6)$$

Rigorously speaking, eq 6 is valid only at infinite dilution. In reality, the motion of diluent, i.e., the solvent, has to be taken into account as follows:[16,17]

$$\Gamma = (1 - \phi)^2 D q^2 \quad (7)$$

The values of the hydrodynamic radius related to the ith mode, $R_{H,i}$, can be evaluated with the following relation:

$$R_{H,i} = \frac{kT}{6\pi\eta_0 D} = \frac{kTq^2}{6\pi\eta_0\Gamma_i} \quad (8)$$

Here, k is the Boltzmann constant and η_0 is the solvent viscosity at temperature T.

The above discussion is valid for ergodic medium, where time average is equal to ensemble average. Most of polymeric systems can be regarded as an ergodic medium. However, polymer gels have nonergodicity due to immobilization of polymer chains introduced by cross-linking as extensively discussed in the literature.[18−21] In the case of a nonergodic medium, the scattered intensity, $I(q)$, varies with sample position because of the lack of ergodicity. Hence, two types of averaging have to be defined to describe the system, i.e., the time average, $\langle I(q)\rangle_T$, and ensemble average, $\langle I(q)\rangle_E$. The intensity distribution, $P(\langle I(q)\rangle_T)$, obeys the following relationship[19]

$$P(\langle I(q)\rangle_T) = H[\langle I(q)\rangle_T - I_F(q)] \exp\left[-\frac{\langle I(q)\rangle_T - I_F(q)}{\langle I(q)\rangle_E - I_F(q)}\right] \quad (9)$$

where $I_F(q)$ is the dynamic component in the scattered intensity, $\langle I(q)\rangle_T$, and $H(x)$ is the Heaviside function, i.e., $H(x) = 0$ for $x < 0$ and $H(x) = 1$ for $x \geq 0$.

Experimental Section

Sample. Poly(2-ethoxyethyl vinyl ether)-*b*-poly(2-hydroxyethyl vinyl ether), PEOVE-*b*-PHOVE, was prepared by living cationic polymerization of 2-ethoxyethyl vinyl ether (EOVE) and 2-(*tert*-butyldimethylsilyloxy)ethyl vinyl ether (BMSiVE), followed by the subsequent conversion of poly(BMSiVE) segments in the precursor block copolymers to PHOVE segments by acid-promoted hydrolysis. The degrees of polymerization of PEOVE and PHOVE were 200 and 400, respectively, determined by gel permeation chromatography. The corresponding PEOVE and PHOVE homopolymers were also prepared for comparison. The details of synthesis were reported elsewhere.[12,22] A prescribed amount of PEOVE-*b*-PHOVE was dissolved in deuterated water (D_2O). It should be noted that there exists a significant isotope effect in phase behavior in polymer blends[23,24] as well as in polymer gels.[25] Therefore, D_2O was chosen as a solvent instead of H_2O even for dynamic light scattering measurement (DLS). The sample solutions were filtered with a 0.20 μm Millipore filter.

DLS. Dynamic light scattering (DLS) experiments were carried out on a static/dynamic compact goniometer (SLS/DLS-5000), ALV, Langen, Germany. A He−Ne laser with 22 mW was used as the incident beam. Nonergodic DLS measurements were conducted with a rotation attachment, ALV, at a fixed angle of 90°. A typical measuring time was 30 s. The temperature of the sample was regulated within an error of ±0.1 °C.

Rheological Measurements. A stress-control-type rheometer (Carri-Med CSL^2 100, TA Instruments) was used to measure the flow properties and dynamic viscoelasticity of the polymer solutions. A cone−plate with a diameter of 4 cm and an angle of 2° was employed. In the case of flow property measurements, after stress was given to the sample within 3 min, and reduced within 3 min, the flow curve was obtained. The shear storage modulus G' and loss modulus G'' were

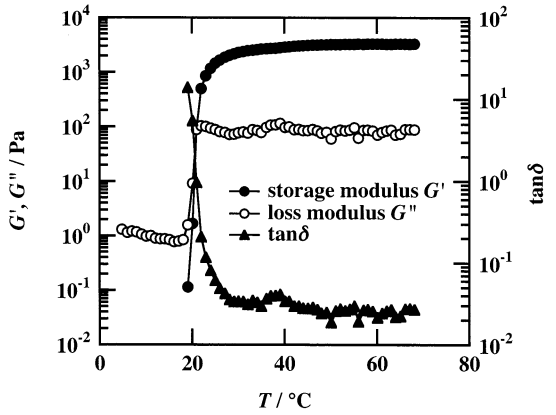

Figure 1. Dynamic mechanical behavior of PEOVE-*b*-PHOVE block copolymer solution at 20 wt % (frequency = 1 Hz). G' = storage moduli, G'' = loss moduli, and tan δ = loss tangent.

measured as a function of frequency, f. Depending on the viscoelastic properties, a suitable shear amplitude, γ, was chosen to ensure the linearity of dynamic viscoelasticity. The temperature of the samples was controlled within 0.1 °C by means of a Peltier element.

Results and Discussion

1. Rheological Measurement. Figure 1 shows dynamic mechanical behavior of PEOVE-*b*-PHOVE aqueous solutions at polymer concentrations of 20 wt %. As shown in the figure, both the storage, G', and loss moduli, G'', increased rapidly at 20 °C. This is due to micellization of PEOVE due to its strong hydrophobicity, followed by a macrolattice formation as evidenced in the previous paper.[12] The PHOVE chains anchored to different micelles interpenetrating to each other, resulting in a drastic increase in viscosity of the system.

Figure 2 shows flow curves of PEOVE-*b*-PHOVE aqueous solutions of 15 wt % at 15.0, 20.5, and 21.0 °C. Surprisingly enough, the change in viscoelasticity is remarkably sharp with respect to temperature. The flow behavior changes within a very limited temperature range, i.e., $19 < T < 20$ °C, from Newtonian flow ($T <$ 19 °C), to non-Newtonian ($T >$ 20.5 °C), and plastic flow behavior ($T >$ 21 °C). In the Newtonian flow region, the shear stress, σ, is proportional to the shear rate, dγ/dt, as follows

$$\sigma = \eta \frac{\mathrm{d}\gamma}{\mathrm{d}t} \tag{10}$$

and the viscosity $\eta = 0.0544$ Pa s. This means that the system is a homogeneous polymer solution. In the non-Newtonian region ($T \approx$ 20.5 °C), on the other hand, the flow behavior suggests that there exists a heterogeneous structure, such as micelles with long hair chains interpenetrating to each other. On the other hand, the rheological behavior in the plastic flow region indicates the presence of a solidlike structure responsible for a yield stress. The flow behavior was given in the following form

$$\sigma \cong \sigma_0 + \eta_a \frac{\mathrm{d}\gamma}{\mathrm{d}t} \tag{11}$$

with the yield stress $\sigma_0 = 45.0$ Pa and the apparent viscosity $\eta_a = 0.140$ Pa s in this particular case. Another interesting feature is absence of significant hysteresis even in the region of the plastic flow. Similar rheological transitions were observed in polystyrene-*b*-polybutadiene in a selective solvent (e.g., *n*-tetradecane; C14).[4,6] It should be noted here, however, the transition of PEOVE-*b*-PHOVE aqueous solutions is much sharper than that of polystyrene-*b*-polybutadiene in C14.

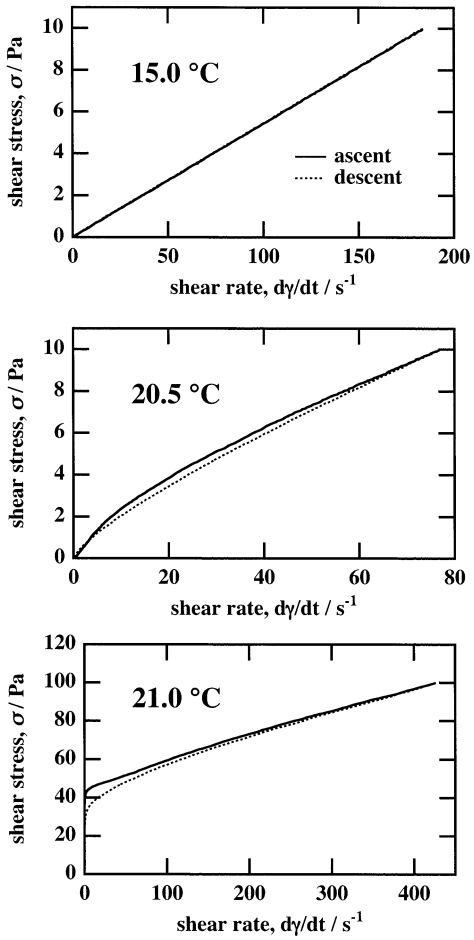

Figure 2. Flow behaviors of PEOVE-*b*-PHOVE in 15 wt % aqueous solution at various temperatures.

Figure 3 shows the frequency, f, dependence of G' and G'' of PEOVE-*b*-PHOVE aqueous solutions at various temperatures. At $T = 19.5$ °C, G' and G'' exhibit typical behavior for viscoelastic (Maxwellian) fluids. That is, G' scales with f^2 and G'' does f^1. At the sol−gel transition threshold, it is known that G' and G'' become collinear with f.[26,27] As a matter of fact, the dynamic mechanical behavior shows G' and $G'' \sim f^{1/2}$ for $f >$ 1 Hz at $T = 21.0$ °C. It is interesting that the G' and G'' functions cross over at $f \approx 1$ Hz. This indicates that this system becomes a viscoelastic fluid with a long relaxation time at this frequency. At a higher frequency than this critical frequency, i.e., $f_c \approx 1$ Hz, the system behaves as a gel. However, for $f < f_c$, it is a viscous solution and flows. At a temperature above the sol−gel transition, both G' and G'' become frequency independent as a typical elastic matter does. In addition, G' is more than 1 order of magnitude larger than G'' in this frequency region, indicating that the loss tangent, tan δ, is less than 0.1. All of these results on rheological properties support structural transition from a nonstructured polymer solution to a macrolattice structure by way of the sol−gel transition.

2. Dynamic Light Scattering (DLS). 2.1. Homopolymers. Figure 4 shows (a) correlation functions (CFs), $g^{(2)}(\tau) - 1$, and (b) cluster distribution functions (CDs), $G(\Gamma)$, of poly(HOVE) in aqueous solution at

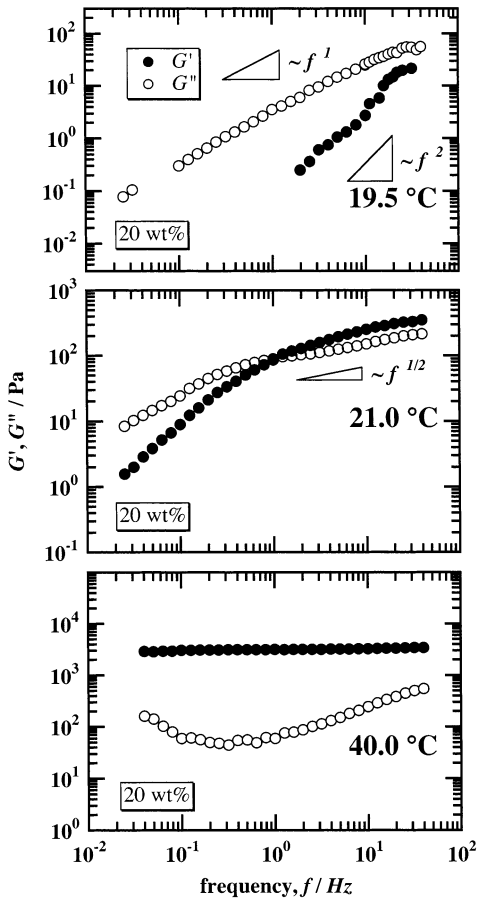

Figure 3. Viscoelastic behavior of PEOVE-*b*-PHOVE in 20 wt % aqueous solution at various temperatures.

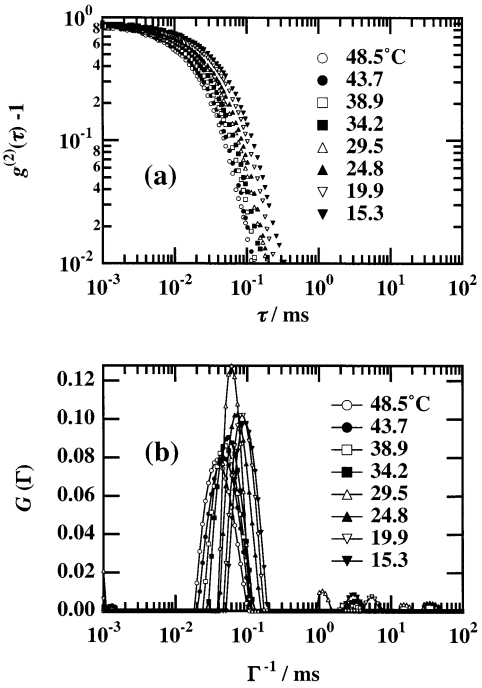

Figure 4. (a) CFs and (b) CDs of PHOVE in aqueous solution at various temperatures.

various temperatures. The polymer concentration was 1.0 wt %. The CF shows existence of single relaxation corresponding to the translational diffusion of PHOVE chains. The characteristic decay time, Γ^{-1}, shifted toward shorter relaxation time. However, this does not mean a contraction of PHOVE chains, but this is due to a decrease in the solvent viscosity with increasing temperature. The variation of R_H with temperature will be discussed in conjunction with that of PEOVE.

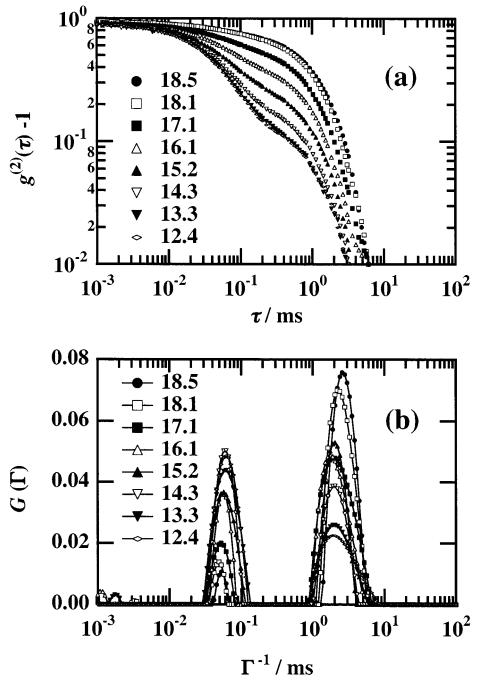

Figure 5. (a) CFs and (b) CDs of PEOVE in aqueous solution at various temperatures. Two relaxation modes appeared assigned to be the fast and slow modes.

Figure 5 shows (a) CFs and (b) CDs of PEOVE in aqueous solution at various temperatures. Because the scattered intensity was very weak, the concentration was increased to 2.0 wt % instead of 1.0 wt %. In contrast to the case of PHOVE, CFs seem to be strongly temperature dependent. Note that there are two peaks in the CDs, i.e., the first, Γ^{-1}_{fast} ($\equiv \Gamma^{-1}_1$), and slow modes, Γ^{-1}_{slow} ($\equiv \Gamma^{-1}_2$). With increasing temperature, Γ^{-1}_{fast} shifts toward shorter relaxation time and its peak height decreased. On the other hand, Γ^{-1}_{slow} moved toward longer relaxation time and the height increased. These correspond to the translational diffusion of individual PEOVE chains and clustered PEOVE chains, respectively. The cluster of PEOVE chains is deduced to be stable enough to keep their size while individual chains have freedom to attach to or detatch from the cluster. Hence, a dynamic equilibrium of the cluster size distribution exists. This is because the clusters are still soluble in water.

Figure 6 shows the variations of (a) R_H of PHOVE, $R_{H,HOVE}$, (b) R_Hs of PEOVE, i.e., $R_{H,EOVE,fast}$ and $R_{H,EOVE,slow}$. Here, we evaluated the values of $R_{H,HOVE}$ with two methods, i.e., from the so-called CONTIN analysis (filled circles) and from the cumulant method (open circles). Both results were in good agreement as shown in the figure. This was the case where only single relaxation mode appeared. However, in the following analysis, we exclusively employed the CONTIN analysis (i.e., with eq 4) because of the presence of multiple relaxation modes which interfered the cumulant analysis. $R_{H,HOVE}$ was rather temperature independent and was about 6.0 nm. In the case of PEOVE, on the other hand, $R_{H,EOVE,fast}$ decreased with T, while $R_{H,EOVE,slow}$ was a strong function of T, particularly for $T \geq 17$ °C. These data indicate that (1) PHOVE chains are molecu-

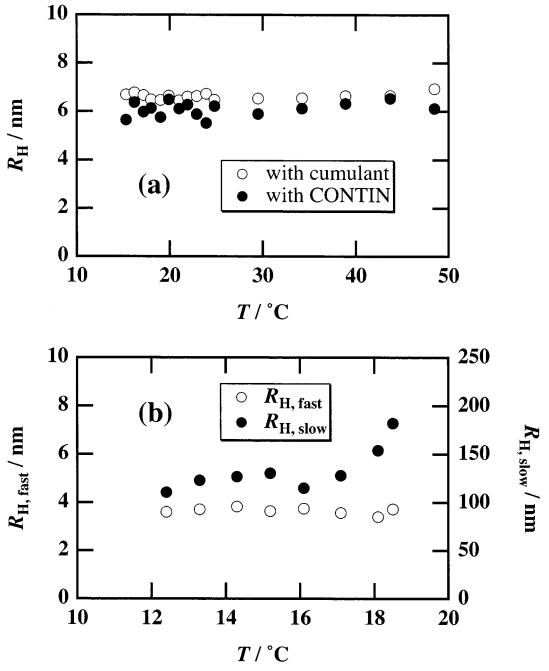

Figure 6. Temperature dependence of (a) R_H for PHOVE (filled circles) and (b) $R_{H,fast}$ (open circles) and $R_{H,slow}$ (filled circles) for PEOVE. The values of R_H for PHOVE were also determined with the cumulant method (open circles).

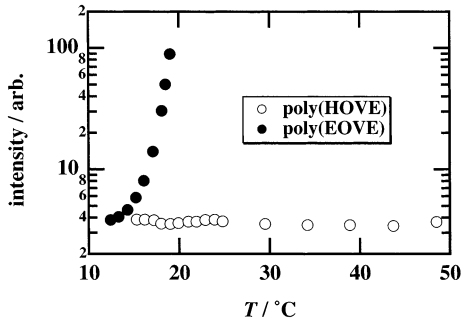

Figure 7. Temperature dependence of $I(q=90°)$ for PHOVE and PEOVE aqueous solutions.

larly dispersed in aqueous solutions at 1 wt % irrespective of temperature and (2) PEOVE chains are in two states, i.e., in molecular dispersion with $R_{H,EOVE,fast} \approx$ 3.6 nm and in clustered state. The size of the clusters, $R_{H,EOVE,slow}$, increased with increasing temperature, particularly for $T \geq 18$ °C. This is due to the fact that the lower critical solution temperature (LCST) of PEOVE in water is located at $T \approx 20$ °C. The invariance of $R_{H,EOVE,fast}$ of PEOVE indicates that contraction does not take place except for the temperature region near LCST, i.e., $T > 18$ °C.

Figure 7 shows the variations of scattered intensity, $I(\theta=90°)$, for (a) 1.0 wt % PHOVE and (b) 2.0 wt % PEOVE solutions, where θ is the scattering angle. As shown in the figure, $I(\theta=90°)$ of PHOVE was temperature independent, while that of PEOVE dramatically increased for $T \geq 17$ °C. This temperature dependence of $I(\theta=90°)$ also indicates that partial clustering takes place exclusively for PEOVE above 17 °C.

2.2. Poly(EOVE-*b*-HOVE). Figure 8 shows (a) CFs and (b) CDs of 1.0 wt % PEOVE-*b*-PHOVE in aqueous solution during a heating process. The temperature was increased stepwise after 30 s measurement and was paused at least 30 min before next measurement.

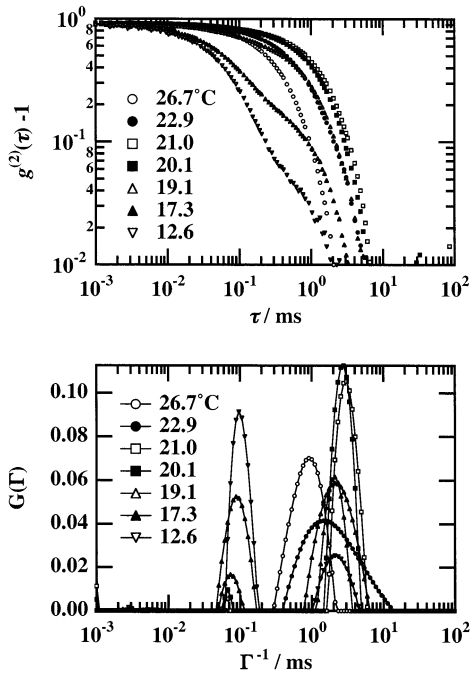

Figure 8. (a) CFs and (b) CDs of 1.0 wt % PEOVE-*b*-PHOVE in aqueous solution.

Though more than 30 CFs were obtained as a function of temperature, only several representative curves are shown in the figure. Similar to the case of PEOVE, there exists two relaxations—one around $\Gamma^{-1}_{fast} \approx 0.1$ ms and the other at $1 \leq \Gamma^{-1}_{slow} \approx 6$ ms at $T = 12.6$ °C. The peak position and height at Γ^{-1}_{fast} decrease with increasing T, while the position, Γ^{-1}_{slow}, of the slow mode was rather strange. At first, Γ^{-1}_{slow} moves toward longer relaxation time. However, Γ^{-1}_{slow} becomes smaller by further increasing T (for $T > 21$ °C). Note that for $T > 21$ °C the fast mode disappears, and the only slow mode survives.

Figure 9 shows (a) the variation of $R_{H,fast}$ and $R_{H,slow}$ and (b) $I(\theta=90°)$ of 1.0 wt % PEOVE-*b*-PHOVE with T. This indicates that micellization took place by anchoring PEOVE chains to a micelle core. As a result, $R_{H,fast}$ decreased and disappeared by increasing T, while $R_{H,slow}$ increased up to $T = 21.0$ °C and then decreased. The decrease of $R_{H,slow}$ is ascribed to formation of stable micelles of ca. 80 nm large in radius including PHOVE corona. In our previous study with small-angle neutron scattering (SANS), the core radius was evaluated to be ca. 20 nm. Hence, this size seems to be consistent with the SANS result.[12] The increase in $R_{H,slow}$ in the temperature region of $18 < T < 21$ °C is deduced to be a transition region from molecular dispersion to micelles, e.g., interconnected chain like structure as will be discussed later. The variation of $I(\theta=90°)$ also indicates such a transition with T. That is, the larger the scattering objects, the larger the scattered intensity. Figure 9b also shows that this structure transition is thermoreversible without significant hysteresis.

Figure 10 shows (a) CFs and (b) CDs of 17 wt % PEOVE-*b*-PHOVE in aqueous solution during a heating process. The scattering angle was 90°. Different from the case of 1 wt % PEOVE-*b*-PHOVE, the CFs exhibits only a slow mode at $\Gamma^{-1} \approx 10^2$ ms for $T \leq 17$ °C. Around 19 °C, CD splits into two peaks, i.e., fast and slow modes. The slower mode is seen at $\Gamma^{-1} \approx 10^2$ ms, while the fast mode is $\Gamma^{-1} \approx 10^1$ ms or less. Another interest-

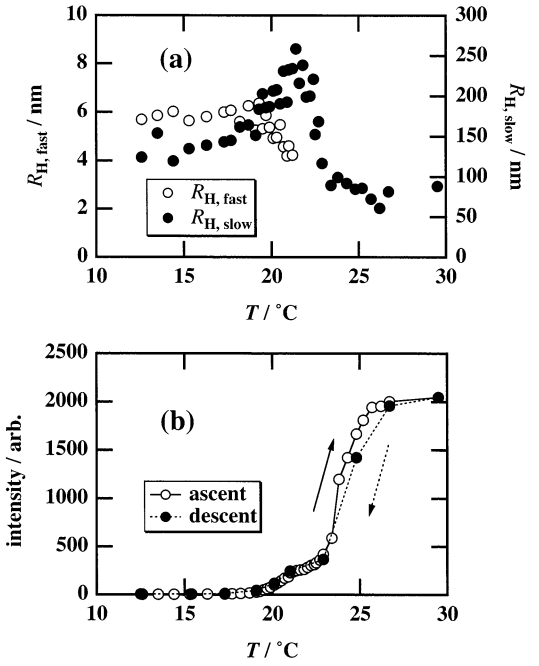

Figure 9. Variation of (a) $R_{H,fast}$, $R_{H,slow}$ and (b) $I(\theta=90°)$ of 1.0 wt % PEOVE-*b*-PHOVE with T.

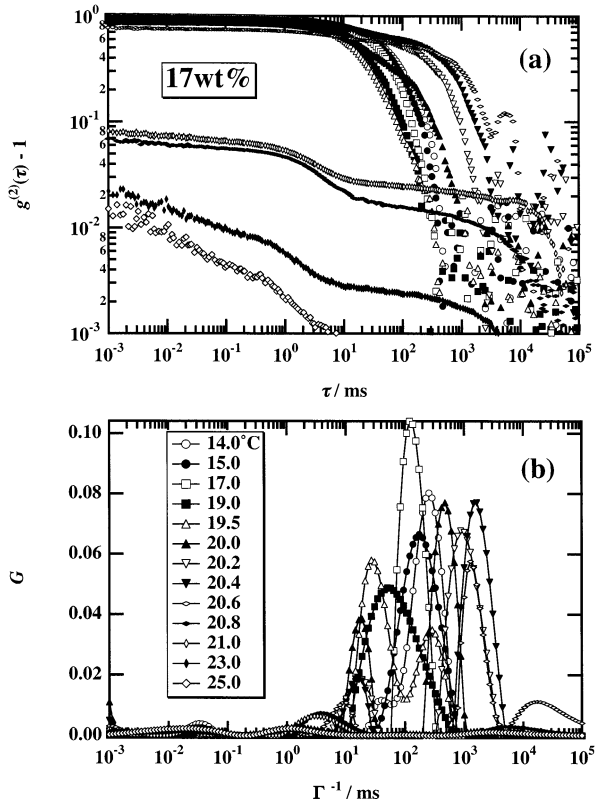

Figure 10. CFs of 17 wt % PEOVE-*b*-PHOVE aqueous solution at various temperatures.

ing feature observed in Figure 10 is the suppression of the initial amplitude of CFs, i.e., $g^{(2)}(\tau=0) - 1$, for $T >$ 20.0 °C. This is an indication of the sol−gel transition.[20]

Figure 11 shows the peak shift of the CDs shown in Figure 10b. This figure clearly indicates that the appearance of the fast mode. With increasing temperature, Γ^{-1} decreased gradually. However, at $T = 19.0$ °C, the peak splits to two, as assigned to be the fast and slow modes. The fast mode kept decreasing to the time range

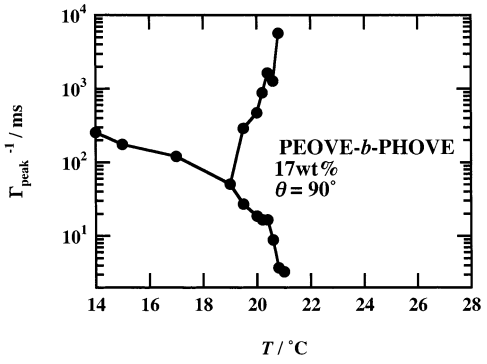

Figure 11. Variation of the characteristic decay time, Γ_{peak}^{-1}, as a function of T. The Γ_{peak}^{-1} splits into two at 19 °C.

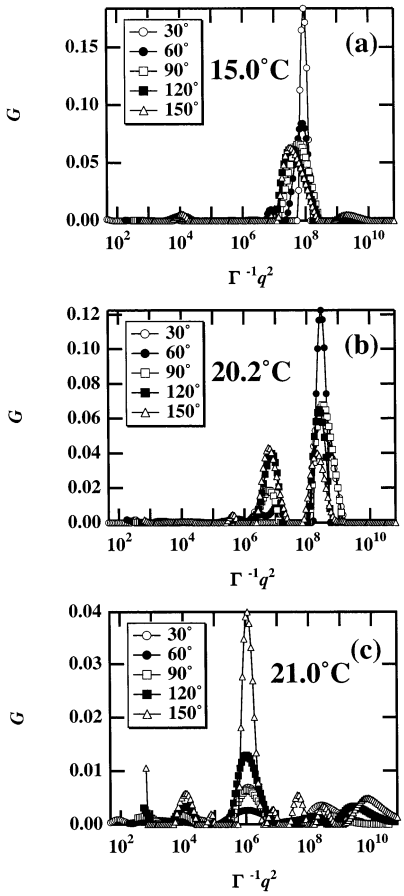

Figure 12. $G(\Gamma^{-1})$ vs $\Gamma^{-1}q^2$ plots of 17 wt % PEOVE-*b*-PHOVE aqueous solution at (a) 15.0, (b) 20.2, and (c) 21.0 °C.

of $\Gamma^{-1} \approx 1$ ms or less, which is of the same order of the so-called "gel mode".[28] Hence, it is deduced that the drastic change of the dynamical property corresponds to the sol−gel transition of the system. As a matter of fact, the 17 wt % PEOVE-*b*-PHOVE aqueous solution exhibited a characteristic flow behavior with a finite value of yield stress, σ_0, at temperatures for $T \geq 21$ °C as shown in Figure 2. In other words, a concentrated PEOVE-*b*-PHOVE solution has a plastic behavior at high temperatures.

To categorize the fast and slow modes, CFs were obtained by varying the scattering angle. Figure 12 shows $G(\Gamma^{-1})$ vs $\Gamma^{-1}q^2$ plots of 17 wt % PEOVE-*b*-PHOVE aqueous solution at (a) 15.0, (b) 20.2, and (c) 21.0 °C. At $T = 15.0$ °C, a single peak appears, and it shifts toward a lower value of $\Gamma^{-1}q^2$ by increasing q. On the other hand, at 20.2 °C, which corresponds to the

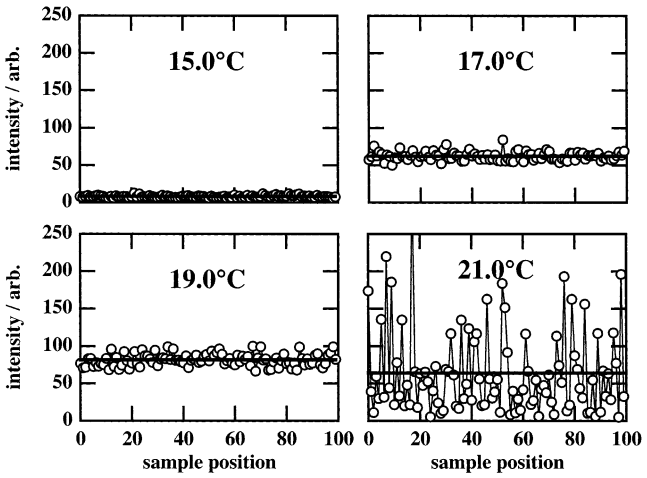

Figure 13. Speckle patterns at various temperatures.

micelle region, there appear two peaks, and they are superimposed to each other irrespective of q. At 21.0 °C, the peak shift even lower value of $\Gamma^{-1}q^2$, but the peaks are again superimposed irrespective of q. Note that the appearance of many peaks is ascribed to the low dynamic correlation by entering a gel phase. This is related to the nonergodic nature of the gel phase as will discussed in the next section.

3. Nonergodic Light Scattering. Figure 13 shows the light scattered intensity from the 17 wt % PEOVE-*b*-PHOVE aqueous solution. A total of 100 sampling positions of a test tube were randomly chosen, and a series of DLS measurements were carried out at various temperatures. At 15 °C, the intensity does not have a noticeable position dependence. Therefore, one can call that this system is ergodic and $\langle I\rangle_T = \langle I\rangle_E$, where $\langle I\rangle_E$ was obtained by averaging $\langle I\rangle_T$ over 100 data points and is shown with the horizontal solid line. With increasing T, $\langle I\rangle_E$ ($= \langle I\rangle_T$) increased and reached a maximum at 19 °C. At 21.0 °C, there appeared strong position dependence in $\langle I\rangle_T$, indicating that the system became nonergodic.

Figure 14 shows the temperature dependence of (a) $\langle I\rangle_E$ and (b) the initial amplitude of the CFs, $g^{(2)}(\tau=0) - 1$, for 17 wt % PEOVE-*b*-PHOVE aqueous solution. At low T's, the scattered intensity was weak, implying that the system is a homogeneous polymer solution. With increasing temperature, on the other hand, the scattered intensity suddenly became strong at about 17 °C, which is identical to the temperature of the formation of micelles determined by the SANS experiment.[12] By further increasing temperature, the intensity slightly decreased and finally leveled off for $T > 20$ °C. Figure 14b shows that an ergodic-to-nonergodic transition took place at 20 °C. It is worth noting that this temperature is not the same as the temperature at which $\langle I\rangle_E$ started to increase or reached a maximum. The ergodic-to-nonergodic transition corresponds to the sol−gel transition, while the latter does to micelle formation. Hence, it can be concluded that DLS measurements are sensitive enough to discriminate the sol−gel transition from the micelle formation transition. Furthermore, these transitions have a one-to-one correspondence to the rheological transitions. That is, micelle formation leads to the Newtonian-to-non-Newtonian transition, and the sol-to-gel transition corresponds to the non-Newtonian-to-plastic flow transition. Another interesting aspect that should be addressed here is that these transitions

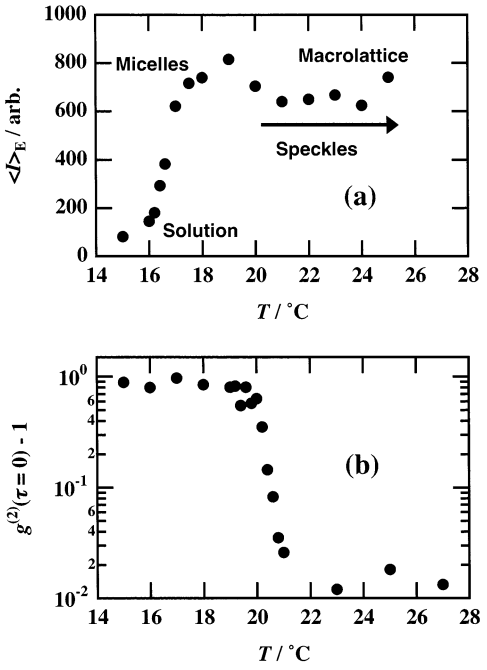

Figure 14. Temperature dependence of (a) $\langle I\rangle_E$ and (b) the initial amplitude of the CFs For 17 wt % PEOVE-*b*-PHOVE aqueous solution.

take place within a very narrow temperature window, i.e., 2−3 °C, which has not been observed in block copolymer−organic solvent systems.[2] Note that PEO-*b*-PPO-*b*-PEO (EO_{97}−PO_{39}−EO_{97}) aqueous solutions require about a 20 °C temperature range (15−36.5 °C for this particular case) for these transitions, where the numbers indicate the number of monomeric unit in a block chain.[8] PS-*b*-PB block copolymers were also reported to have a wide temperature range of about 20−30 °C for these transitions.[4−6] The sharp structure transitions found in PEOVE-*b*-PHOVE are ascribed to the strong temperature dependence of the interaction parameter of PEOVE with water, of which the origin has to been elucidated in more detail.

4. Structural Transition of PEOVE-*b*-PHOVE in Aqueous Solutions. As discussed in the previous sections, PEOVE-*b*-PHOVE undergoes two transitions by increasing temperature. One is the molecular dispersion-to-micelle transition and the other the sol-to-gel transition. The latter transition was confirmed to be the micelle-to-macrolattice transition by SANS. These transitions are schematically depicted in Figure 15a−c. However, this is the case of concentrated solutions. In a dilute PEOVE-*b*-PHOVE solutions (e.g., 1 or 2 wt %) (Figure 15d), on the other hand, only PEOVE chains coagulate and form a micellar structure (Figure 15f) with increasing temperature. Note here that this micelle formation proceeds via an intermediate state with extremely slow relaxation time. Though a direct observation on this intermediate state has not been carried out, an interconnected chain cluster, depicted as Figure 15e, may be formed, and this structure is responsible for the very slow relaxation observed for 1.0 wt % PEOVE-*b*-PHOVE aqueous solutions at $20 < T < 22$ °C.

Conclusion

DLS and rheological studies have been carried out on aqueous solutions of PEOVE-*b*-PHOVE, where PEOVE is the thermosensitive polymer and PHOVE is the

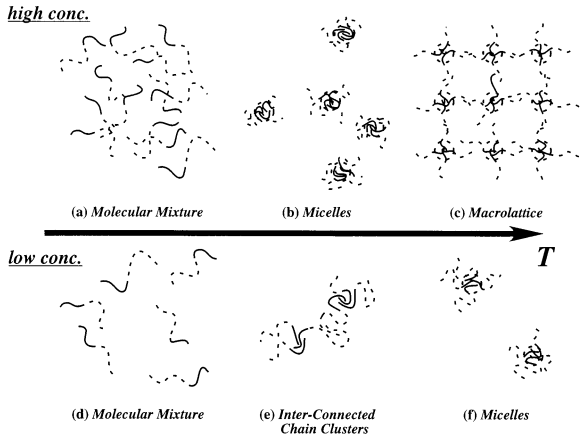

Figure 15. Schematic representation of showing two transitions from the molecular dispersion (a) to the crystal-like structure with macrolattice (c) by way of the micellar structure (b) in concentrated PEOVE-*b*-PHOVE aqueous solution. Parts d−f show the case of dilute PEOVE-*b*-PHOVE aqueous solution, where the intermediate state is deduced to be an interconnected chain cluster structure.

hydrophilic polymer. DLS measurements for the corresponding homopolymer solutions suggested that the hydrodynamic radius of PHOVE, $R_{H,HOVE}$, is around 6 nm and is temperature independent. On the other hand, a strong clustering was observed for PEOVE with increasing temperature. At low temperatures, the cluster size distribution function CDs showed two distinct peaks, corresponding to the fast (individual molecule) and slow modes (clusters). The value of $R_{H,fast}$ was initially 3.7 nm at 12.6 °C, but because of clustering, the relaxation mode corresponding to the individual molecules disappeared for $T > 17$ °C and gigantic clusters of the order of 200 nm are formed around LCST of PEOVE, which finally precipitate. The DLS results for PEOVE-*b*-PHOVE aqueous solutions were similar to those of PEOVE and exhibited a strong temperature dependence. Two-step structural transitions were observed, which are (I) the molecular dispersion-to-micelles and (II) the micelles-to-macrolattice transition. These behaviors are well correlated to the drastic changes in the rheological properties, i.e., Newtonian, non-Newtonian, and plastic flow. DLS measurements were successfully employed to discriminate these transitions as (I) a drastic increase in the scattered intensity and change in the hydrodynamic radius and (II) appearance of speckle pattern and suppression of the initial value of correlation functions. The temperature window required for these transitions were only a few degrees Celsius, which is much narrower than those for block copolymers in organic solvent. This is one of the characteristic features of aqueous systems containing polyampholytes because of the strong temperature dependence of hydrophobic interaction.

Acknowledgment. This work is partially supported by the Ministry of Education, Science, Sports and Culture, Japan (Grant-in-Aid, 13031019, 14045216, and 14350493 to M.S.).

References and Notes

(1) Molau, G. E. In *Block Polymers*; Aggarwal, S. L., Ed.; Plenum Press: New York, 1970.
(2) Hamley, I. W. *The Physics of Block Copolymers*; Oxford University Press: Oxford, 1998.
(3) Helfand, E.; Wasserman, Z. R. In *Developments in Block Copolymers*; Goodman, I., Ed.; Applied Science: New York, 1982.
(4) Watanabe, H.; Kotaka, T.; Hashimoto, T.; Shibayama, M.; Kawai, H. *J. Rheol.* **1982**, *26*, 153.
(5) Shibayama, M.; Hashimoto, T.; Kawai, H. *Macromolecules* **1983**, *16*, 16.
(6) Hashimoto, T.; Shibayama, M.; Kawai, H.; Watanabe, H.; Kotaka, T. *Macromolecules* **1983**, *16*, 361.
(7) Mortensen, K. *Prog. Colloid Polym. Sci.* **1993**, *93*, 72.
(8) Mortensen, K. *Prog. Colloid Polym. Sci.* **1993**, *91*, 69.
(9) Mortensen, K.; Brown, W. *Macromolecules* **1993**, *26*, 4128.
(10) Aoshima, S.; Sugihara, S. *J. Polym. Sci., Part A: Polym. Chem.* **2000**, *38*, 3962.
(11) Sugihara, S.; Matsuzono, S.; Sakai, H.; Abe, M.; Aoshima, S. *J. Polym. Sci., Part A: Polym. Chem.* **2001**, *39*, 3190.
(12) Okabe, S.; Sugihara, S.; Aoshima, S.; Shibayama, M. *Macromolecules* **2002**, *35*, 8139.
(13) Chu, B. *Laser Light Scattering*, 2nd ed.; Academic Press: New York, 1991.
(14) Siegert, A. F. J. *MIT Radiation Report* **1943**, *465*.
(15) Schulz-DuBoir, E. O. In *Photon Correlation Techniques in Fulid Mechanics*; Schulz-DuBoir, E. O., Ed.; Springer-Verlag: Berlin, 1983; p 15.
(16) Edwards, S.; Miller, A. G. *J. Phys. C: Solid State Phys.* **1976**, *9*, 2011.
(17) Vink, H. *J. Chem. Soc., Faraday Trans. 1* **1985**, *81*, 1725.
(18) Pusey, P. N.; van Megen, W. *Physica A* **1989**, *157*, 705.
(19) Joosten, J. G. H.; McCarthy, J. L.; Pusey, P. N. *Macromolecules* **1991**, *24*, 6690.
(20) Shibayama, M. *Macromol. Chem. Phys.* **1998**, *199*, 1.
(21) Furukawa, H.; Hirotsu, S. *J. Phys. Soc. Jpn.* **2002**, *71*, 2873.
(22) Aoshima, S.; Hashimoto, K. *J. Polym. Sci., Part A: Polym. Chem.* **2001**, *39*, 746.
(23) Yang, H.; Hadziioannou, G.; Stein, R. S. *J. Polym. Sci., Polym. Phys. Ed.* **1983**, *21*, 159.
(24) Yang, H.; Shibayama, M.; Stein, R. S.; Shimizu, N.; Hashimoto, T. *Macromolecules* **1986**, *19*, 1667.
(25) Shibayama, M.; Tanaka, T.; Han, C. C. *J. Chem. Phys.* **1992**, *97*, 6829.
(26) Winter, H. H.; Chambon, F. *J. Rheol.* **1986**, *30*, 367.
(27) Winter, H. H.; Mours, M. *Adv. Polym. Sci.* **1997**, *134*, 167.
(28) Tanaka, T. In *Dynamic Light Scattering*; Pecora, R., Ed.; Plenum Publishing: New York, 1985; pp 347−362.

MA030066P